

Building a High-Resolution Velocity Model with Full-Waveform Inversion: A Case Study for Soda Lake Geothermal Field

Kai Gao and Lianjie Huang

Geophysics Group, Los Alamos National Laboratory, Los Alamos, NM 87545

kaigao@lanl.gov, ljh@lanl.gov

Keywords: Full-waveform inversion, Soda Lake geothermal field, high-resolution velocity model

ABSTRACT

Full-waveform inversion is becoming a powerful tool to build high-resolution subsurface velocity models. Previous studies reveal that the Soda Lake geothermal field, situated several miles north-west of Fallon in Nevada, contains a complex fault system and complex geological structures. Therefore, it is a great challenge to build a high-resolution velocity model for the Soda Lake geothermal field using conventional tools such as migration velocity analysis. We have recently developed a suite of novel full-waveform inversion methods for high-resolution velocity inversion in complex media. We apply one of our methods to surface seismic data acquired at the Soda Lake geothermal field to build a high-resolution velocity model. Our full-waveform inversion employs a wavefield-energy normalization preconditioning technique and a modified total-variation regularization scheme to accelerate the convergence rate of the inversion and improve the recovery of sharp interfaces. Our results show that this inversion method can recover more fine-scale velocity variations compared with those built using migration velocity analysis. The high-resolution velocity model obtained using full-waveform inversion could improve imaging of the complex fault system at the Soda Lake geothermal field.

1. INTRODUCTION

Accurate imaging of subsurface structures is important for geothermal energy exploration and reservoir characterization. Full-wavefield-based imaging methods such as reverse-time migration (RTM) usually improve migration images, yet require accurate, high-resolution subsurface velocity models (e.g., Baysal et al., 1983; Tan and Huang, 2014). Velocity models are often obtained using migration velocity analysis (MVA) or full-waveform inversion (FWI). MVA (e.g., Biondi and Symes, 2004) estimates the internal velocity in the image domain by iteratively measuring the coherency of migration images, and the resulting velocity model of MVA is a “macromodel” – a smooth velocity model that is suitable for seismic migration. On the other hand, FWI (e.g., Tarantola, 1984) uses both the amplitude and traveltimes information of seismic wavefields by iteratively reducing the difference between synthetic and recorded seismic data. It is therefore possible to obtain small-scale/high-resolution structures using FWI. A challenge faced in FWI is that field seismic data usually lack of low-frequency contents, and therefore it is difficult for FWI to converge efficiently and reliably (to the global minimum of the misfit function).

In this study, we produce a high-resolution velocity model for the Soda Lake geothermal field in Nevada using a recently developed FWI with a modified total-variation (MTV) regularization scheme (Lin and Huang, 2015). We apply this FWI-MTV method to 3D active surface seismic data acquired at the Soda Lake geothermal field. We use a smooth velocity model obtained using MVA as the initial velocity model for our FWI-MTV inversion. We employ a two-stage/multi-scale FWI-MTV inversion scheme to produce a high-resolution velocity model. We first conduct the FWI-MTV inversion using the smooth MVA velocity model and a relatively low-frequency bandpass filtered seismic data with a center frequency of 20 Hz to obtain an inverted velocity model. We then continue the FWI-MTV inversion starting from this initially inverted velocity model and relatively high-frequency bandpass filtered seismic data with a center frequency of 40 Hz to produce a high-resolution velocity model.

This paper is organized as follows. We briefly describe the FWI-MTV method, present some necessary pre-processing procedures to improve the convergence of FWI, and show the inverted high-resolution velocity model for the Soda Lake geothermal field and the convergence history of the FWI-MTV inversion.

2. METHODOLOGY

2.1 FWI-MTV

FWI-MTV minimizes the following misfit functional iteratively (Lin and Huang, 2015):

$$E(\mathbf{m}, \mathbf{u}) = \|\mathbf{d} - f(\mathbf{m})\|^2 + \lambda_1 \|\mathbf{m} - \mathbf{u}\|^2 + \lambda_2 \|\mathbf{u}\|_{TV}, \quad (1)$$

where \mathbf{d} is the field seismic data, $f(\mathbf{m})$ is the synthetic seismic data under model \mathbf{m} , $\|\mathbf{d} - f(\mathbf{m})\|^2$ is the L_2 -norm of the data misfit term, $\|\mathbf{m} - \mathbf{u}\|^2$ is the L_2 -norm Tikhonov regularization term, $\|\mathbf{u}\|_{TV}$ is the L_1 -norm total-variation (TV) regularization term, λ_1 and λ_2 are the regularization parameters for Tikhonov and TV regularization terms, respectively. Minimization problem (1) is further decomposed into two sub-problems and solved using an alternating direction method of minimizer (Lin and Huang, 2015), i.e., in the k -th iteration,

$$\begin{cases} \mathbf{m}^{(k)} = \arg \min_{\mathbf{m}} E_1(\mathbf{m}) = \arg \min_{\mathbf{m}} \{ \|\mathbf{d} - f(\mathbf{m})\|^2 + \lambda_1 \|\mathbf{m} - \mathbf{u}^{(k-1)}\|^2 \}, \\ \mathbf{u}^{(k)} = \arg \min_{\mathbf{u}} E_2(\mathbf{u}) = \arg \min_{\mathbf{u}} \{ \|\mathbf{m}^{(k)} - \mathbf{u}\|^2 + \lambda_2 \|\mathbf{u}\|_{TV} \}. \end{cases} \quad (2)$$

This MTV minimization scheme can preserve sharp interfaces of the model and improve the robustness of FWI. In addition, we apply the wavefield-energy preconditioning method to FWI-MTV to accelerate the inversion convergence rate (Zhang et al., 2012).

2.2 Data and initial model preparation

We use 3D surface seismic data acquired at the Soda Lake geothermal field in Nevada for velocity model building with FWI-MTV. A data processing company process the 3D seismic data using denoising, automatic gain control (AGC), surface wave removal, etc. We further process the data to make them suitable for full-waveform inversion.

2.2.1 Remove the amplitude distortion caused by AGC

To invert seismic data for a high-resolution velocity model using FWI, it is necessary for the seismic data to have correct amplitude information, yet the AGC distorts the amplitude information by boosting the later-arrival signals reflected from the deep layers and geological structures. Therefore, we apply a reverse AGC procedure to the seismic data to recover the original wavefield amplitudes. We find that this procedure can effectively improve the convergence of FWI inversion.

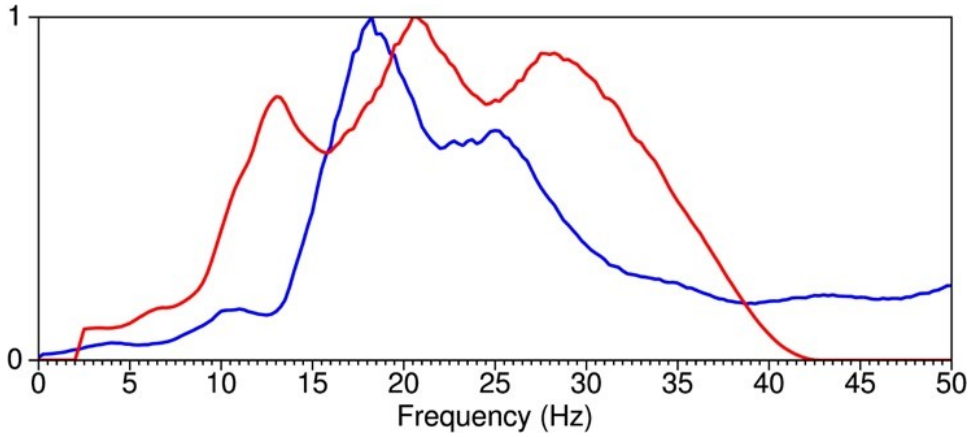


Figure 1: Comparison between the normalized average frequency spectrum of the original data (blue curve) and that of a filtered data (red curve).

2.2.2 Frequency-domain data filtering

The original seismic data acquired at the Soda Lake geothermal field have spectra with a wide frequency range. The blue curve in Fig. 1 displays the average frequency spectrum of the denoised seismic data, showing that the dominant frequency is around 20 Hz, while there are some amount of frequency contents that are higher than 45 Hz. These high-frequency contents in the seismic data are useful in exploring small-scale structures at the Soda Lake geothermal field. To improve the convergence of the FWI-MTV inversion of the Soda Lake seismic data and avoid the local minima of the misfit function, we employ a multi-scale inversion scheme. For the first stage of the FWI-MTV inversion, we apply inversion only to the low-frequency contents of seismic data. Therefore, we filter the Soda Lake seismic data using a low-pass filter with a 45 Hz cut-off frequency, and the red curve in Fig. 1 depicts the resulting normalized average frequency spectrum.

In addition to the aforementioned two data processing procedures, we also resample or downsample the smooth velocity model derived from MVA to 6.7 m in all three spatial dimensions using spline interpolation, as shown in Fig. 2 for a 2D slice of the 3D velocity model. We use this model as the initial velocity model for the first-stage FWI-MTV inversion.

A good estimation of the source wavelet (including the amplitude and the temporal signature) is essential to obtain accurate FWI results. We make an estimation of the source amplitude by comparing numerically simulated reflection signals with the field seismic reflection signals from the top of the high-velocity body as depicted in Fig. 2. We also determine the center frequency of the source wavelet by analyzing the spectra of all seismic data. The center frequency for the first-stage FWI-MTV inversion is 20 Hz, and that for the second stage FWI-MTV inversion is 40 Hz.

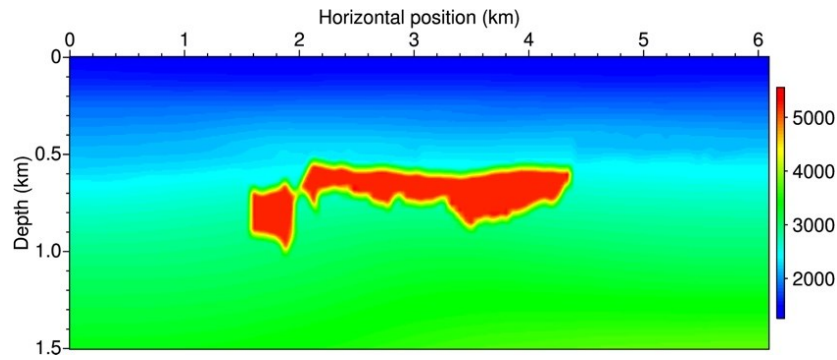


Figure 2: Initial P-wave velocity model derived from MVA of 3D seismic data acquired at the Soda Lake geothermal field. The P-wave velocity of the high-velocity body is approximately 5500 m/s.

3. RESULTS

2.1 First-stage FWI-MTV inversion

Our first-stage FWI-MTV inversion uses low-frequency bandpass filtered seismic data with relatively low-frequency contents as discussed in the proceeding section, and uses the MVA velocity model as shown in Fig. 2 as the initial velocity model. Except the interface between the high-velocity body and the smooth background velocity model, there are no sharp interfaces in the initial model. After 30 FWI iterations, the normalized relative data misfit decreases to about 88% of the initial data misfit value; and the inversion partially reconstruct the layers in the shallow region of the model (shallower than 500 m). Figure 3 shows the inverted velocity model after 30 iterations. Figure 4 displays the convergence history for this first-stage FWI-MTV inversion. The velocity update in the central part of the model (1.5~4.5 km in horizontal position and 0~0.6 km in the vertical direction) shows complex geological structures and discontinuous layers. This is consistent with the Kirchhoff time and depth migration images. In these images, this region of the Soda Lake geothermal field contains a complicated fault system where the faults have various strikes and dip angles. It is therefore difficult for us to obtain model updates with clear and continuous interfaces for this region of the model.

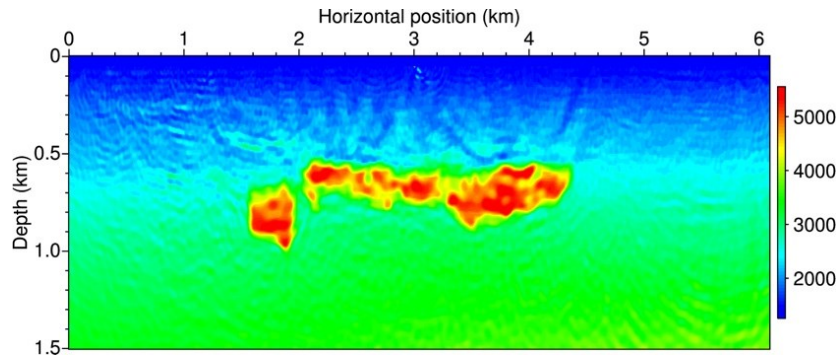


Figure 3: Inverted P-wave velocity model after 30 iterations in the first-stage FWI-MTV inversion. Note the obvious improvements in the shallow region (<0.5 km) of the model.

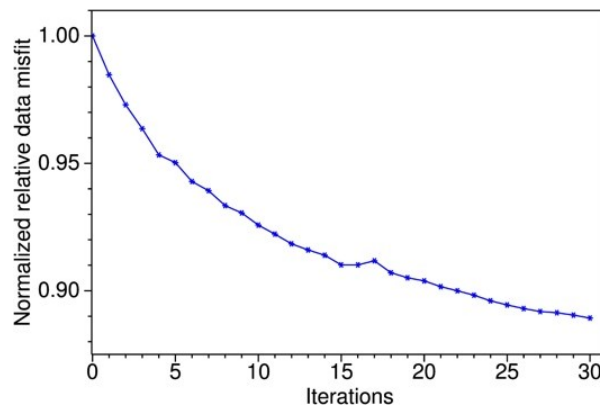


Figure 4: Convergence history of the first-stage FWI-MTV inversion in 30 iterations. The relative data misfit is normalized to 1.

The deep region of the model, particularly the region beneath the high-velocity body in the center of the Soda Lake velocity model, is poorly updated because of the imperfect reverse AGC process as well as limited illumination. Nevertheless, we can still observe some improvements in Fig. 3 compared with Fig. 2 at depth deeper than 0.5 km, particularly at horizontal positions smaller than 1 km and greater than 5 km.

Note that we do not enforce velocity update constraints at the high-velocity body, resulting in some velocity changes inside the high-velocity body compared to Fig. 2. Actually, the homogeneous high-velocity body is only an approximation and simplification. The well logs show that there is certain level of velocity variations inside the high-velocity region.

2.2 Second-stage FWI-MTV inversion

The second-stage FWI-MTV inversion uses the updated velocity model of the first-stage FWI-MTV inversion after 30 iterations (Fig. 3) as the initial velocity model. We perform 50 iterations for the second-stage FWI-MTV inversion, and Fig. 5 depicts the updated velocity model. Figure 6 displays the normalized relative data misfit that decreases to about 65% of the initial value.

Compared to the initial velocity model in Fig. 3, the inverted velocity model of the second-stage FWI-MTV inversion of seismic data with higher frequencies shows more continuous layers, particularly in the shallower region of the model at depth smaller than 0.25 km. At horizontal positions greater than 4.5 km and at depth 0.3~0.4 km, the interfaces and layers are more obviously continuous than those in Fig. 3. Meanwhile, at horizontal positions smaller than 1 km, some of the continuous structures disappear and are replaced by some discontinuous structures in Fig. 5, which indicates that there might be some complicated faults penetrate into this region of the Soda Lake model. The second-stage FWI-MTV inversion also updates the fault system in the central shallow part. At least two faults become more obvious: one around horizontal position 2.8~2.9 km, one around horizontal position 4.2~4.5 km. There are also some updates of several dipping layers around horizontal position 3.6~4.4 km at depth about 0.4 km.

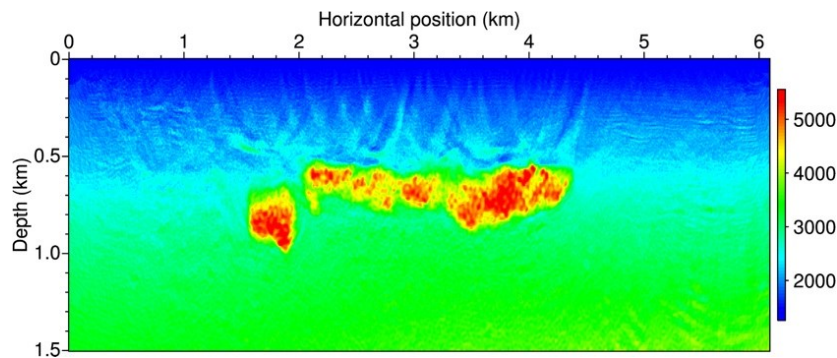


Figure 5: Inverted P-wave velocity model after 50 iterations in the second-stage FWI-MTV inversion using the velocity model in Fig. 3 as the initial model.

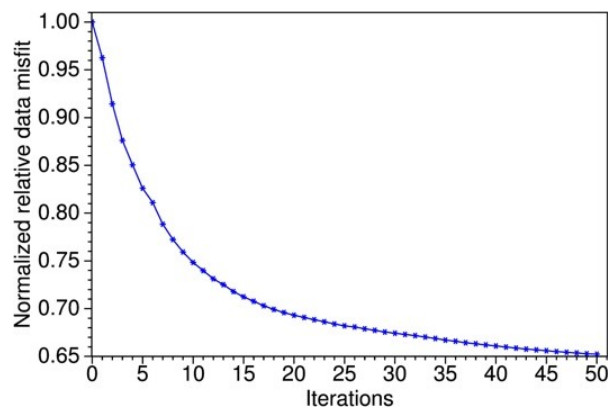


Figure 6: Convergence history of the second-stage FWI-MTV inversion in 50 iterations. The relative data misfit is normalized to 1.

4. CONCLUSIONS

We have obtained a high-resolution velocity model for the Soda Lake geothermal field using a multi-scale full-waveform inversion method with modified total-variation regularization. The inversion procedure consist of two stages. The first stage uses a smooth velocity model derived from migration velocity analysis as the initial model, and the second stage of inversion employs the updated velocity model in the first-stage inversion as the initial model. The full-waveform inversion can also use using more scales/stages. The final inverted velocity model shows clear improvements over the initial smooth model. For example, the final inversion result reveals continuous layers, faults and some small-scale structures. These features do not exist in the initial smooth initial model, particularly in the shallow region of the model at depth smaller than 0.5 km. Future work includes building complete 3D P- and S-wave velocity models and possible anisotropic parameter models for the Soda Lake geothermal field to improve characterization of the geology and reservoir characteristics of the field.

5. ACKNOWLEDGEMENTS

This work was supported by the Geothermal Technologies Office of the U.S. Department of Energy through contract DE-AC52-06NA25396 to Los Alamos National Laboratory. The computation was performed on super-computers provided by the Institutional Computing Program of Los Alamos National Laboratory.

REFERENCES

- Baysal, E., Kosloff, D., and Sherwood, J., Reverse-time migration: *Geophysics*, **48**, (1983), 1514–1524.
- Biondi, B. and Symes, W., Angle-domain common-image gathers for migration velocity analysis by wavefield-continuation imaging: *Geophysics*, **69**, (2004), 1283–1298.
- Lin, Y., and Huang, L., Acoustic- and elastic-waveform inversion using a modified total-variation regularization scheme: *Geophysical Journal International*, **200**, **1**, (2015), 489–502.
- Tan, S. and Huang, L., Least-squares reverse-time migration with a wavefield-separation imaging condition and updated source wavefields: *Geophysics*, **79**, (2014), S195-S205.
- Tarantola, A., Inversion of seismic reflection data in the acoustic approximation: *Geophysics*, **49**, (1984), 1259–1266.
- Zhang, Z., Huang, L., and Lin, Y., 2012, A wave-energy-based precondition approach to full-waveform inversion in the time domain: *SEG Technical Program Expanded Abstracts*, 82nd Annual International Meeting, Las Vegas, NV, (2012).